NIH Public Access
Author Manuscript
J Agric Food Chem. Author manuscript; available in PMC 2011 January 27.

Published in final edited form as:
J Agric Food Chem. 2010 January 27; 58(2): 1040–1045. doi:10.1021/jf902854y.

Isolation and Identification of Triglycerides and Ester Oligomers from Partial Degradation of Potato Suberin

Weimin Wang[†], **Shiying Tian**[†], and **Ruth E. Stark**[*,†,§]

[†]Department of Chemistry, College of Staten Island, City University of New York Graduate Center and Institute for Macromolecular Assemblies, New York, NY 10031

[§]Department of Chemistry, City College of New York, City University of New York Graduate Center and Institute for Macromolecular Assemblies, New York, NY 10031

Abstract

Suberized cell walls from wound-healing potato tubers (*Solanum tuberosum*) were depolymerized under mild conditions using methanolic potassium hydroxide in order to investigate the chemical linkages present in this protective plant biopolymer. Analysis of the resulting soluble oligomeric fragments with HPLC, 1D and 2D NMR, LC/MS and MS^n methods allowed identification of several novel compounds: a family of homologous triglycerides, a family of homologous aliphatic ester trimers, and an ether linked phenylacetic acid dimer. These findings illustrate the diversity of rigid and flexible molecular linkages present in both poly(aliphatic) and poly(aromatic) domains of potato suberin, and they point toward architectures that may account for its function as a potent hydrophobic barrier to water, thermal equilibration, and microbial pathogens.

Keywords

potato; *Solanum tuberosum*; suberin; polyester; triglyceride; triacylglycerol; NMR; 2D NMR; MS

INTRODUCTION

Much as cuticles protect the leaf and fruit surfaces of terrestrial plants, suberized cells serve an analogous function within internal tissues and in wound periderms. In particular, these polymeric assemblies have common roles in enabling the plant to control water egress and ingress, providing thermal insulation, and offering a physical barrier to pathogenic attack (1–4). The suberin biopolyester is a familiar constituent of cork and tree bark as well as the end product of stress response to potato tuber skinning injury. Significant structural insight into this material has resulted from the characterization of its monomeric degradation products and of intact suberized cell walls (1–4), including recently reported approaches using enzymatic hydrolysis (5) and solubilization in ionic liquids (6). Nonetheless, a full molecular description has remained elusive because suberin can be confused with lignin, is impossible to examine independently of the cell walls in which it is deposited, and cannot be dissolved readily or crystallized.

It is now established that suberin comprises physically distinct polyaliphatic and polyphenolic domains that may be linked internally and/or to each other by glycerol ester bridges (7,8), though direct evidence for their supramolecular architecture remains sparse. Glycerol itself was reported as a suberin monomer more than a half century ago (9); it has been isolated more

*To whom correspondence should be addressed: Tel: 212-650-8916. FAX: 212-650-8719. stark@sci.ccny.cuny.edu.

NIH-PA Author Manuscript
NIH-PA Author Manuscript
NIH-PA Author Manuscript

NIH-PA Author Manuscript

NIH-PA Author Manuscript

NIH-PA Author Manuscript

recently among the depolymerization products from oak, cotton, cork, and potato tissues (10–15) and monitored quantitatively in parallel with the suberization process (15). Moreover, partial methanolysis has revealed the presence of functionalized glycerol products: monoacylglycerol esters of alkanoic acids, ω-hydroxy fatty acids, hydroxycinnamoyl-glyceryl esters, and α,ω-diacids, as well as a diglycerol ester linked to α,ω-diacids at both ends (8). Glycerol, α,ω-diacids, and monoacylglycerol esters have also been reported as molecular constituents of related plant materials including waxes in suberized cotton fibers (7) and *Arabidopsis thaliana* epidermal tissues (16,17). The possibility of glycerol linkages between the aliphatic and phenolic domains is consistent with the report of monoferuloylglycerol in wound healing potato tubers (10,18).

In the current study of suberin from potato wound periderm, we identified new aliphatic and aromatic products from partial depolymerization. These new findings are discussed in the context of the reported building blocks of this protective biopolymer, current hypotheses regarding the supramolecular arrangement of suberin in plant tissues, and its ultimate regulatory and structural functions.

MATERIALS AND METHODS

Chemicals

Double-processed tissue culture water, *A. niger* pectinase (EC 3.2.1.15), sodium acetate, and tristearin (1,2,3-trioctadecanoylglycerol) were obtained from Sigma Chemical Company (St. Louis, MO). *Aspergillus niger* cellulase (EC 3.2.1.4) was purchased from ICN (Aurora, OH). Solvents for Soxhlet extraction (methanol, methylene chloride, chloroform) were purchased from Aldrich (Milwaukee, WI). HPLC grade acetonitrile, methanol, water, isopropanol (IPA), *n*-butanol, hexane, and acetone, as well as formic acid, ammonium formate, and trifluoroacetic acid (TFA) were purchased from Fisher (Fair Lawn, NJ). $CDCl_3$ (99.98%) was purchased from Cambridge Isotope Laboratories (Andover, MA).

Isolation of potato suberin

Potato tubers (*Solanum tuberosum* L. cv. Russet Burbank) were purchased from a local supermarket. Suberization of wounded potatoes and isolation of the suberized cell walls followed published procedures (19–21): (1) peeling, wounding, and incubating the potato tissue disks for 7 d at 25±0.1 °C under sterile conditions; (2) enzymatic removal of unsuberized cell walls with successive cellulase and pectinase treatments; (3) exhaustive dewaxing by sequential Soxhlet extraction with refluxing methylene chloride and methanol/methylene chloride (1:1 v/v). Approximately 200 g of peeled potatoes yielded 2 g of suberized potato periderm tissue.

Chemical depolymerization of potato suberin

After optimizing for the yield of oligomeric and phenolic products, suberin was partially degraded using 0.5–1.5 M solutions of methanolic KOH solution at room temperature for 0.5–4 h. Then the reacted mixtures were acidified to pH 4–5 with concentrated HCl. The acidified mixture was filtered to remove the resulting KCl salt, and the methanol solvent was evaporated to obtain the monomer and oligomer products. The dried materials were taken up in a chloroform/methanol (1:1 v/v) mixture for subsequent chromatographic separation.

Isolation of triglycerides, ester oligomers, and aromatic ethers from potato suberin

For preliminary separation, the extracted suberin alkaline hydrolysis products were subjected to silica gel 60 column chromatography (Mallinckrodt Baker, Paris, KY) and eluted using a step gradient of hexane, acetone and methanol solvents. About 40% by weight of the product

NIH-PA Author Manuscript

NIH-PA Author Manuscript

NIH-PA Author Manuscript

mixture was eluted in a single fraction that was rich in ester and aromatic groups as judged by ^{1}H nuclear magnetic resonance (NMR) (see below). After successive extractions guided by ^{1}H NMR monitoring, the methanol-insoluble portion yielded trimeric ester oligomers; the methanol-soluble triglycerides were further purified using a Hewlett-Packard Model 1100 high performance liquid chromatography (HPLC) instrument (Agilent, Santa Clara, CA) equipped with a quaternary solvent delivery system and UV, diode array, and evaporative light scattering (Alltech, Burtonsville, MD) detectors. The column used was a 50 mm×4.6 mm i.d., 3.5 μm, Symmetry Shield RP-8 (Waters Corporation, Millford, MA). The mobile phase program consisted of a linear gradient from 70 to 100% MeOH (0.04% TFA) over 10 min at a flow rate of 0.9 mL/min, followed by a 2.0 min hold at 100% MeOH (0.04% TFA). A tristearin standard (Sigma) was prepared by dissolving in chloroform and diluting with IPA. The standard and purified samples were injected into an HPLC for LC/mass spectrometry (LC/MS) and LC/MS^{n} analysis. Aromatic ethers were purified from the chromatographic fraction described above by TLC and subsequent HPLC using a hexane/isopropanol/acetic acid mobile phase that decreased over 33 min at a flow rate of 0.5 mL/min from 99.3:0.5:0.2 to 91.5:8.3:0.2 (v/v).

Solution-State NMR Spectroscopy

NMR spectra of the successively solvent-extracted products were acquired on a Varian ^{UNITY}INOVA spectrometer (Palo Alto, CA) operating at ^{1}H and ^{13}C frequencies of 599.95 and 150.87 MHz, respectively. Depolymerized suberin samples were dissolved in $CDCl^{3}$ to provide a field-frequency lock signal and contained 1% tetramethylsilane to provide an internal chemical shift standard (Aldrich). One- and two-dimensional spectra were acquired using a Varian HCN probe equipped with pulsed field gradients and optimized for ^{1}H detection. Data processing and ^{1}H peak integration were done with VNMR software; ^{1}H and ^{13}C chemical shift predictions were derived using database software from Advanced Chemistry Development (Toronto, Canada).

To establish through-bond connectivities within and between monomer units of the oligomers, a variety of two-dimensional NMR experiments were used. Pairs of through-bond coupled ^{1}H nuclei were identified by proton correlation spectroscopy (COSY). Directly bonded proton-carbon pairs were found from gradient-assisted heteronuclear single quantum coherence (gHMQC) spectroscopy (22) using a polarization transfer time corresponding to $^{1}J_{CH}$ = 140 Hz. Finally, long-range proton-carbon interactions were delineated using heteronuclear multiple bond correlation (gHMBC) spectroscopy (23) with a polarization transfer time corresponding to $^{3}J_{CH}$ = 10 Hz, unless noted otherwise. Additional experimental conditions have been described elsewhere (24).

Mass Spectrometry

Mass spectrometric data were acquired on Agilent Technologies 1100 Series LC/MSD Trap SL or G1946D systems (Santa Clara, CA). Atmospheric pressure chemical ionization (APCI), atmospheric pressure photoionization (APPI), and electrospray ionization (ESI) were carried out in both positive and negative ion modes with the following conditions: for APCI and APPI, an HPLC flow rate of 400–1000 μL/min, drying gas temperature of 300 °C, nebulizer pressure of 60 psi, and drying gas flow rate of 5 L/min; for ESI, 200 °C, 30 psi, and 13 L/min. Mass spectra were obtained by scanning from *m/z* 100 to 2000, using a capillary voltage of 4000 V. Since no molecular ions were observed using the customary methanol-water system, ammonium formate was added to the mobile phase to promote formation of an ammonium adduct ($[M+18]^{+}$) in the MS experiments. For LC/MS^{n} analysis of both the tristearin standard and triglycerides isolated from potato suberin, samples were eluted from HPLC with a 1:1 (v/v) mixture of two solvents (25): water:isopropanol (60:40) + 25 mM ammonium formate (A); water:isopropanol:*n*-butanol (10:10:80) + 25 mM ammonium formate (B). For LC/MS of ester

NIH-PA Author Manuscript

NIH-PA Author Manuscript

NIH-PA Author Manuscript

oligomers, elution was done isocratically with a 1:1 (v/v) mixture of solvents A and B at a flow rate 0.9ml/min. The resulting data were processed using Agilent ChemStation software.

RESULTS AND DISCUSSION

Potato suberin depolymerization and product isolation

Suberin-enriched potato cell wall materials were isolated from wound-healing tissues as described previously (19). The chemical degradation reaction was optimized to balance the total yield of soluble products with the proportions of aromatic and esterified target compounds by varying the depolymerization time (15 min – 3 d) and KOH concentration (0.5 – 1.5 M), as described previously for tomato cutins (26); the optimized time range was 0.5 – 4 h. Both the mass of unreacted suberized potato tissue and the intensity of diagnostic ^{1}H NMR resonances (4.03 ppm, ester bonds; 6–8 ppm, aromatics) with respect to **CH_2**C=O's (2.28 ppm) were used to make this assessment. Overall yields of the soluble products from potato wound periderm were 7–14%, consistent with the range of 5–40% reported for chemical degradation of suberized cell walls from various sources (1,5,6,10) and ≥50% for diverse fruit cutins (24, 27–29). Although primarily monomers were obtained under all reaction conditions, the largest yields of oligomer-rich product fractions from preliminary chromatographic purification were obtained after ~ 0.5 h of reaction time, which was used in subsequent experiments. Neither the overall nor oligomer yields were sensitive to KOH concentration.

Structural analysis of suberin triacylglycerols: overview

Glycerol, which has been reported previously as a constituent in suberin from potato peels and wound periderm (2,10,11), was identified from its 1D (^{1}H) and 2D (HMQC, HMBC) NMR spectra, which showed the expected chemical shifts and through-bond connectivities. Four triglyceride mixtures (**1**–**4**) that were isolated chromatographically 186 as described above were elucidated by APCI-MS and NMR methods. Molecular weights were fit to the formula M = A-18 = 218.03 + 28.03m + 26.02n, where A is the mass of the observed NH_4^+ 189 adduct ion in MS, M is the molecular weight, 218.03 accounts for the glycerol-carboxiloxy moiety plus three methyl groups, m is the number of ethylene groups, and n is the number of ethenyl groups. As none of the fractions displayed ^{1}H NMR signals corresponding to multiply bonded structures, it was assumed that n = 0. Both MS and NMR data obtained for the isolated triacylglycerols were in full accord with results for authentic glycerol tristearate (tristearin).

APCI-MS of the respective fractions (numbered according to their elution order) yielded adduct ions corresponding to $[M+18]^+$ as follows: **1**, *m/z* 419.3, 488.4, and 544.4; **2**, *m/z* 516.4; **3**, *m/z* 488.4, 656.7, 684.7, 740.7, 768.8, 784.8,and 796.8; **4**, 488.5, 600.5, 656.5, 684.8, 740.8, 768.8, 796.8, 824.8, 852.6, and 908.4. MS data for these mixtures, which contain primarily triglycerides, are summarized in Table 1. Although the near-identical polarity of the close homologs largely precluded chromatographic isolation of pure compounds, it was possible to verify the expected trend toward slower elution times for the less polar compounds that have longer acyl chains.

To distinguish the possible chain-length combinations and deduce which fatty acid chains are esterified to each position of the glycerol backbone, MS^n data were collected and compared to fragmentation patterns of a triglyceride standard. MS^n experiments also provided clean parent-to-daughter analysis of each pure compound in a mixture. From the ammonium adduct ion of tristearin at *m/z* 909.0, a fragment at 607.6 was observed in MS^2, and further broken down in MS^3 to an ion at 267.2. The proposed tristearin fragmentation pathway is shown in Figure 1, where it is reasonable to assume that steric considerations allow more facile cleavage at positions 1 and 3 to yield more stable secondary ions. For the depolymerization products

NIH-PA Author Manuscript

NIH-PA Author Manuscript

NIH-PA Author Manuscript

described below, it was assumed that all members of a homologous series had similar MS^n fragmentation patterns.

NMR analysis of triacylglycerols

A common spectroscopic signature was observed for both the tristearin standard and successively solvent-extracted degradation products. The ^1H spectra each displayed multiplets at 5.24, 4.28, and 4.13 ppm corresponding to CHO on the 2-chain and each pair of inequivalent CH_2 groups on chains 1 and 3; integrated intensity ratios were 1:4 for CHO:CH_2O of tristearin and 1:5 for mixtures that contained additional ester oligomers (identified provisionally below). No signals corresponding to multiply bonded moieties were observed. The chemical shifts and covalent bonding patterns derived from 2D NMR are summarized in Table 2 with reference to the structure in Figure 2. All ^1H and ^{13}C chemical shifts were in excellent agreement with ACD spectral simulations.

Through-bond connections involving the backbone and acyl chains, which made it possible to analyze the dominant triglyceride structures even when an ester oligomer component was present in the same mixture, were established by several means. First, COSY NMR established homonuclear correlations between each pair of resonances at 4.13, 4.28 and 5.24 ppm, showing that the three groups are bonded together. In gHMQC, the proton signals at 4.13 and 4.28 ppm (x, z and x', z') were each directly linked to a carbon at 61.9 ppm; the adjacent carbon (y) must be tertiary to render protons x and x', z and z' inequivalent. The (5.24, 68.8 ppm) correlation observed for the CHO group (y) is consistent with a downfield shift due to the oxygen. In gHMBC (see Supplementary Materials), crosspeaks between the ^{13}C resonance at 172.9 ppm and ^1H signals at 4.13 and 4.28 ppm were diagnostic for ester bonds (24,30), namely correlations between protons from the hydroxyl side with the carbonyl carbon. The carbonyl at 172.9 ppm was also correlated with protons at 2.28 ppm from the carboxyl side of the ester. Additionally, the ^1H signals at 4.13 and 4.28 ppm showed the expected HMBC correlations to the CHO carbon resonating at 68.8 ppm. The gHMBC crosspeaks at (4.13, 61.9 ppm) and (4.28, 61.9 ppm) were at first confounding because those correlations had been identified in gHMQC with a (COO-**CH2**)$_2$-CH-O- moiety, but in fact they correspond to 3-bond connectivities for $H_{zz'}$-C_x and $H_{xx'}$-C_z in the symmetric triglyceride backbone structure. Finally, the HMBC crosspeak at (5.24, 172.7 ppm) implicated an ester moiety of a secondary alcohol; adjustment of the gHMBC delay time to match a small ^3J value (23,31) boosted the modest signal intensity of the crosspeak to this single 'y' proton. Moreover, adjustment of the HMBC conditions revealed that the ester carbonyls were correlated to (x, x') and (z, z') protons resonating at (4.03, 4.26) and (4.12, 4.28) ppm, supporting subtle structural differences between the attached alkyl chains (data not shown).

Structural analysis of triacylglycerols: 2

From the ammonium adduct ion of HPLC-isolated fraction **2** at *m/z* 516.4, fragments at 355.3 and 327.3 were observed in MS^2; further fragmentation of 355.3 yielded ions at 155.1 and 127.2 in MS^3, whereas further fragmentation of 327.3 yielded an ion at 127.2 (see Supplementary Materials). Following a scheme analogous to the tristearin standard, it was possible to find two positional isomers (Figure 3) with the (8, 8, 10) chain-length combination for which the proposed MS fragmentation pathways are consistent with the observed mass spectrometric data (Figure 4). However, it was not possible to determine whether the unique 10-carbon chain was located at the 1,3 or 2 positions because the standard triglyceride produced fragments with identical chain length. The identification of **2** was supported by NMR spectral data as detailed above.

NIH-PA Author Manuscript

NIH-PA Author Manuscript

NIH-PA Author Manuscript

Structural analysis of triacylglycerols: 1

As noted above, molecular ions ($[M+ NH4]^+$) appeared in the APCI-MS spectrum at *m/z* 419.3, 488.4 and 544.5. The latter two adducts corresponded to homologous triglyceride structures for which structural analysis followed **2** described above; they were confirmed by MS^n spectra in which 488.4 lost two successive C_8 fragments to yield peaks at *m/z* 327.3 and 127.2, whereas 544.5 fragmented in three possible ways: by losing a C_8 and then a C_{10} fragment to yield peaks at *m/z* 383.3 and 155.1; by losing a C_{10} and then a C_8 fragment to yield peaks at *m/z* 355.3 and 155.1; or by losing two successive C_{10} fragments to yield peaks at *m/z* 355.3 and 127.1. Thus **1** contains a triglyceride with three C_8 chains (M corresponding to 28 less, i.e., one CH_2CH_2 smaller than **2**) and a homolog with a C_8 and two C_{10} chains (M of 28 more, i.e., one CH_2CH_2 larger than **2**). These identifications were consistent with the NMR data.

Structural analysis of triacylglycerols: 3 and 4

Although APCI-MS of **3** yielded multiple molecular ions ($[M+ NH_4]^+$) at *m/z* 488.4, 656.7, 684.7, 740.7, 768.8, 796.8, and 784.8, these triglycerides were simply homologs with various combinations of 10- to 16- carbon chains. A similar situation applied to the methanol-insoluble fraction **4**, for which APCI-MS gave ions ($[M+ NH_4]^+$) at *m/z* 488.4, 600.5, 656.6, 684.7, 740.7, 768.8, 796.8, 824.8, 852.6, and 908.7. The listed chain combinations (including tristearin) shown in Table 1 were verified by conducting MS^2 and MS^3 experiments (data not shown) interpreted with the fragmentation pathway demonstrated for the tristearin standard.

Provisional structural analysis of aliphatic ester oligomers and aromatic ethers

Successive solvent extraction also yielded an oligomeric fraction with architecture similar to those found in fruit cutins (24,30). ^{1}H NMR displayed diagnostic resonances for esters (-C**H$_2$**OC(O)-, 4.05 ppm and -C**H$_2$**COO-, 2.26 ppm), long-chain methylenes (-C**H$_2$**)$_n$-, 1.24 and 1.6 ppm), primary alcohols (-C**H$_2$**OH, 3.62 ppm), and methyl groups (-C**H$_3$**, 0.85 ppm). Crosspeaks observed in the 2D spectra supported the key assignments: (-**CH$_2$**OC(O)-, 4.05, 63.8 ppm) and (-**CH2**OH, 3.62, 62.9 ppm) in gHMQC; -C**H$_2$O**C(O)- , 4.05, 173.6 ppm in gHMBC. The NMR spectra did not provide evidence for mid-chain carbonyl or hydroxyl groups, but doubly bonded moieties were present in a partially characterized fraction from the same separation scheme (data not shown).

These structural identifications assisted with the interpretation of APCI-MS data, which are summarized in Table 3. As described above for the triglycerides (**2**), a homologous series of compounds was present (Figure 5). Isotopic peaks ($[M+1]^+$) that were ~60% as intense as the main molecular ions suggested trimer ester structures, and two additional assumptions were made: as in neutral fats, the chains are of similar length; and, as in aliphatic monomers from cork or potato suberin (2), the carbon chain lengths lie in the range of 14 to 18. The molecular weights derived from $[M+H]^+$, $[M-H]^-$, and $[M+NH_4]^+$ ions in MS were consistent with either CH_3,OH or CH_3,CH_3 molecular termini; since protons are not lost easily from methyl groups, the CH_3,CH_3 structure was deduced for compounds that exhibited only positive ions in APCI.

Finally, a novel ether-linked aromatic compound absorbing in the UV/Vis spectrum at 260 nm was identified by NMR and MS methods. The ^{1}H NMR spectrum included aromatic resonances (7.97 ppm (d), 7.48 ppm (t), and 7.33 ppm (t)), oxygenated aliphatics (4.48 ppm (t) and 3.87 ppm (t), and the familiar diagnostic signals for esters (-C**H$_2$**OC(O)-, 4.01 ppm and -C**H$_2$**COO-, 2.28 ppm). 2D COSY spectra verified pairwise interactions between the aromatics and between the oxygenated aliphatics, whereas gHMQC supported these assignments: phenyl rings (7.97, 129.7 ppm; 7.48, 132.9 ppm; 7.33, 128.4 ppm) and oxymethylenes (4.48, 63.7 ppm; 3.87, 68.9 ppm). Covalent linkages of both the phenyl rings and oxymethylenes to a carboxyl group were revealed by gHMBC crosspeaks at (7.97, 166.7 ppm and 4.48, 166.7 ppm). The gHMBC crosspeak at (3.87, 68.9 ppm) was initially surprising because it matched a correlation identified

NIH-PA Author Manuscript

NIH-PA Author Manuscript

NIH-PA Author Manuscript

in gHMQC, but both observations may be accommodated by a symmetric ether flanked by carboxylate groups: Ph-COO-CH_2-CH_2-O-CH_2-CH_2-OOC-Ph, where the HMBC peak corresponds to 3-bond connectivities 'across' the ether oxygen. This proposal was in excellent agreement with ACD spectral simulations and was confirmed by MS data corresponding to a molecular weight of 314 and molecular formula $C_{18}H_{18}O_5$. Ions corresponding to $[M+H]^+$ at *m/z* 315 were observed in APCI, APPI, and ESI MS experiments, and the last type of ionization also produced several adducts consistent with this mass: $[M+NH_4]^+$ at *m/z* 332, $[M+Na]^+$ at *m/z* 337, and $[2M+Na]^+$ at *m/z* 651.

DISCUSSION

This report firstly offers new insights into the long-enigmatic molecular architecture of suberin from potato wound periderm. The family of suberin triglycerides reported herein adds to known glycerol-based structures such as monoacylglycerol esters of alkanoic acids, ω-hydroxy fatty acids, and α,ω-diacids, hydroxycinnamoyl-glyceryl esters and a diglycerol ester linked to α,ω-diacids at both ends (7,8,10). Our findings demonstrate esterification at all three glycerol sites to form triglyceride structures, possibly in the layers or lamellae of the suberin poly (aliphatic) domain (SPAD) (2). We found no evidence for the monoacylglycerols and diglycerol alkenedioates reported previously by Graça and Pereira (8,10), possibly because those investigators used CaO and $Ca(OH)_2$-catalyzed methanolysis of a suberin from potato periderm; even more likely, our NMR-guided isolation procedures could have bypassed possible glyceride products that each amounted to <0.03 % of the soluble product mixture and displayed different ester CH_2O NMR resonances than the major triglyceride products. The triglycerides identified herein include the C_{16} and C_{18} homologs typical of previously reported suberin monomers but also many medium-chain (C_8–C_{12}) species with saturated aliphatic chains, suggesting distinct biosynthetic origins. Moreover, the triglycerides contain no chemical moieties capable of covalent linkage to other parts of the suberin polymeric structure, leaving the hypothesis of glycerol bridges between polyaliphatic and polyphenolic domains of suberin unconfirmed. Nonetheless, the triglyceride aliphatic chains, together with homologous associated waxes, could form a potent hydrophobic barrier to water and microbial attack at wound surfaces, whether associated physically or bound covalently to the remainder of the suberin polymer.

Secondly, the provisional identification of a family of aliphatic ester trimers underscores both the architectural similarities and differences between suberin and cutin plant biopolymers. Whereas linear esters of hydroxy fatty acids are common among the oligomeric building blocks of fruit cutins (24,28), the typical midchain hydroxyl groups of many of these oligomers are absent in our suberin hydrolysis products. This result is reasonable in light of divergent cutin and suberin biosynthesis (2). The predominance of C_{18} homologs and ω-hydroxyalkanoic acid building blocks is consistent with previously reported suberin monomers and could promote effective hydrophobic interactions with analogous acyl chain structures present in the SPAD.

Thirdly, the aromatic dimer structure deduced from NMR and MS data illustrates an additional ether bridging motif between aromatic esters that could provide short but flexible molecular linkages within the suberin poly(phenolic) domain. Together, these findings add intriguing new pieces to the evolving molecular puzzle of this important protective plant material.

Supplementary Material

Refer to Web version on PubMed Central for supplementary material.

NIH-PA Author Manuscript

NIH-PA Author Manuscript

NIH-PA Author Manuscript

ABBREVIATIONS

COSY	proton correlation spectroscopy
HMQC	heteronuclear single quantum coherence
HMBC	heteronuclear multiple bond correlation
APCI	atmospheric pressure chemical ionization
APPI	atmospheric pressure photoionization
ESI	electrospray ionization
LC/MS_n	liquid chromatography – tandem mass spectrometry
SPAD	suberin poly(aliphatic) domain
SPPD	suberin poly(phenolic) domain

Acknowledgments

We gratefully acknowledge Dr. Hsin Wang for assistance with the setup and optimization of the 2D NMR experiments, Dr. Daniel Arrieta-Baez for valuable consultation on the depolymerization and structural elucidation procedures, and Dr. Subhasish Chatterjee for sharing expertise for the preparation of figures. Dr. Cliff Soll ran several essential experiments at the CUNY/Hunter College MS Facility.

Financial Support. This work was supported by grants MCB-0134705, MCB-0815631, and MCB-0843627 from the U.S. National Science Foundation. The NMR and LC/MS Facilities are operated by the College of Staten Island, Hunter College, and the CUNY Institute for Macromolecular Assemblies, a Center of Excellence of the Generating Employment through New York State Science Program. Additional infrastructural support was provided at The City College of New York by NIH 5G12 RR03060 from the National Center for Research Resources.

LITERATURE CITED

1. Kolattukudy PE. Polyesters in higher plants. Adv. Biochem. Eng. Biotechnol 2001;71:1–49. [PubMed: 11217409]
2. Bernards MA. Demystifying suberin. Can. J. Bot 2002;80:227–240.
3. Graca J, Santos S. Suberin: the biopolyester of plants' skin. Macromolecular Bioscience 2007;7:128–135. [PubMed: 17295399]
4. Franke R, Schreiber L. Suberin -- a biopolyester forming apoplastic plant interfaces. Curr. Opin. Plant Biol 2007;10:252–259. [PubMed: 17434790]
5. Jarvinen R, Silvestre A, Holopainen U, Nyyssoola A, Gil AM, Neto CP, Lehtinen P, Buchert J, Kaltia S. Suberin of potato (*Solanum tuberosum* var. Nikola); comparison of the effect of cutinase CcCut1 hydrolysis with chemical depolymerization. J. Agric. Food Chem 2009;57:9016–9027. [PubMed: 19739639]
6. Mattinen M-L, Filpponen I, Jarvinen R, Li B, Kallio H, Lehtinen P, Argyropoulos D. Structure of the polyphenolic component of suberin isolated from potato (*Solanum tuberosum* var. Nicola). J. Agric. Food Chem 2009;57:9747–9753.
7. Schmutz A, Jenny T, Ryser U. A caffeoyl-fatty acid-glycerol ester from wax associated with green cotton fibre suberin. Phytochemistry 1994;36:1343–1346.
8. Graca J, Pereira H. Diglycerol alkenedioates in suberin: building units of a Poly(acylglycerol) Polyester. Biomacromolecules 2000;1:519–522. [PubMed: 11710176]
9. Ribas I, Blasco E. Investigaciones sobre el corcho. I. Sobre la existencia de glicerina. Ann. R. Soc. Esp. fis. Quim 1940;36B:141–147.
10. Graça J, Pereira H. Suberin structure in potato periderm: glycerol, long-chain monomers, and glyceryl and feruloyl dimers. J. Agric. Food Chem 2000;48:5476–5483. [PubMed: 11087505]
11. Moire L, Schmutz A, Buchala A, Yan B, Stark RE, Ryser U. Glycerol is a suberin monomer. New experimental evidence for an old hypothesis. Plant Physiol 1999;119:1137–1146. [PubMed: 10069853]

NIH-PA Author Manuscript

NIH-PA Author Manuscript

NIH-PA Author Manuscript

12. Graça J, Pereira H. Methanolysis of bark suberins: analysis of glycerol and acid monomers. Phytochem. Anal 2000;11:45–51.
13. Schmutz A, Jenny T, Amrhein N, Ryser U. Caffeic acid and glycerol are constituents of the suberin layers in green cotton fibres. Planta 1993;189:453–460.
14. Rosa E, Pereira H. The effect of long-term treatment at 100–150 C on structure, chemical composition and compression behaviour of cork. Holzforschung 1994;48:226–232.
15. Bento M, Pereira H, Cunha M, Moutinho A, van den Berg K, Boon J. Thermally assisted transmethylation gas chromatography-mass spectrometry of suberin components in cork from *Quercus suber* L. Phytochem. Anal 1998;9:1–13.
16. Bonaventure G, Beisson F, Ohlrogge J, Pollard M. Analysis of the aliphatic monomer composition of polyesters associated with *Arabidopsis* epidermis: occurrence of octadeca-cis-6,cis-9-diene-1,18-dioate as the major component. Plant J 2004:920–930. [PubMed: 15584957]
17. Pollard M, Beisson F, Li Y, Ohlrogge J. Building lipid barriers: biosynthesis of cutin and suberin. TRENDS Plant Sci 2008;13:236–246. [PubMed: 18440267]
18. Bernards MA, Lewis NG. Alkyl ferulates in wound healing potato tubers. Phytochemistry 1992;31:3409–3412. [PubMed: 11536514]
19. Pacchiano RA, Sohn W, Chlanda VL, Garbow JR, Stark RE. Isolation and spectral characterization of plant cuticle polyesters. J. Agric. Food Chem 1993;41:78–83.
20. Bernards MA, Lopez ML, Zajicek J, Lewis NG. Hydroxycinnamic acid-derived polymers constitute the polyaromatic domain of suberin. J. Biol. Chem 1995;270:7382–7386. [PubMed: 7706282]
21. Yan B, Stark RE. A WISE NMR approach to heterogeneous biopolymer mixtures: dynamics and domains in wounded potato tissues. Macromolecules 1998;31:2600–2605.
22. Muller L. Sensitivity enhanced detection of weak nuclei using heteronuclear multiple quantum coherence. J. Am. Chem. Soc 1979;101:4481–4484.
23. Bax A, Summers MF. ^{1}H and ^{13}C assignments from sensitivity-enhanced detection of heteronuclear multiple-bond connectivity by 2D multiple quantum NMR. J. Am. Chem. Soc 1986;108:2093–2094.
24. Tian S, Fang X, Wang W, Yu B, Cheng X, Qiu F, Mort AJ, Stark RE. Isolation and identification of oligomers from partial degradation of lime fruit cutin. J. Agric. Food Chem 2008;56:10318–10325. [PubMed: 18828637]
25. Mcintyre D. The analysis of triglycerides in edible oils by APCI LC/MS. Agilent Application Note. 2000 5968-0878E.
26. Osman SF, Irwin PL, Fett WF, O'Connor JV, Parris N. Preparation, isolation, and characterization of cutin monomers and oligomers from tomato peels. J. Agric. Food Chem 1999;47:799–802. [PubMed: 10563971]
27. Walton TJ, Kolattukudy PE. Determination of the structures of cutin monomers by a novel depolymerization procedure and combined gas chromatography and mass spectrometry. Biochemistry 1972;11:1885–1896. [PubMed: 5025631]
28. Holloway PJ. Cutins of *Malus pumila* fruits and leaves. Phytochemistry 1973;12:2913–2920.
29. Gerard HC, Osman SF, Fett WF, Moreau R. Separation, identification, and quantification of monomers from cutin polymers by high-performance liquid chromatography and evaporative light-scattering detection. Phytochem. Anal 1992;3:139–144.
30. Fang X, Qiu F, Yan B, Wang H, Mort AJ, Stark RE. NMR studies of molecular structure in fruit cuticle polyesters. Phytochemistry 2001;57:1035–1042. [PubMed: 11423150]
31. Bovey, FA.; Jelinski, LW.; Mirau, PA. Nuclear Magnetic Resonance Spectroscopy. San Diego: Academic Press; 1988.

NIH-PA Author Manuscript

NIH-PA Author Manuscript

NIH-PA Author Manuscript

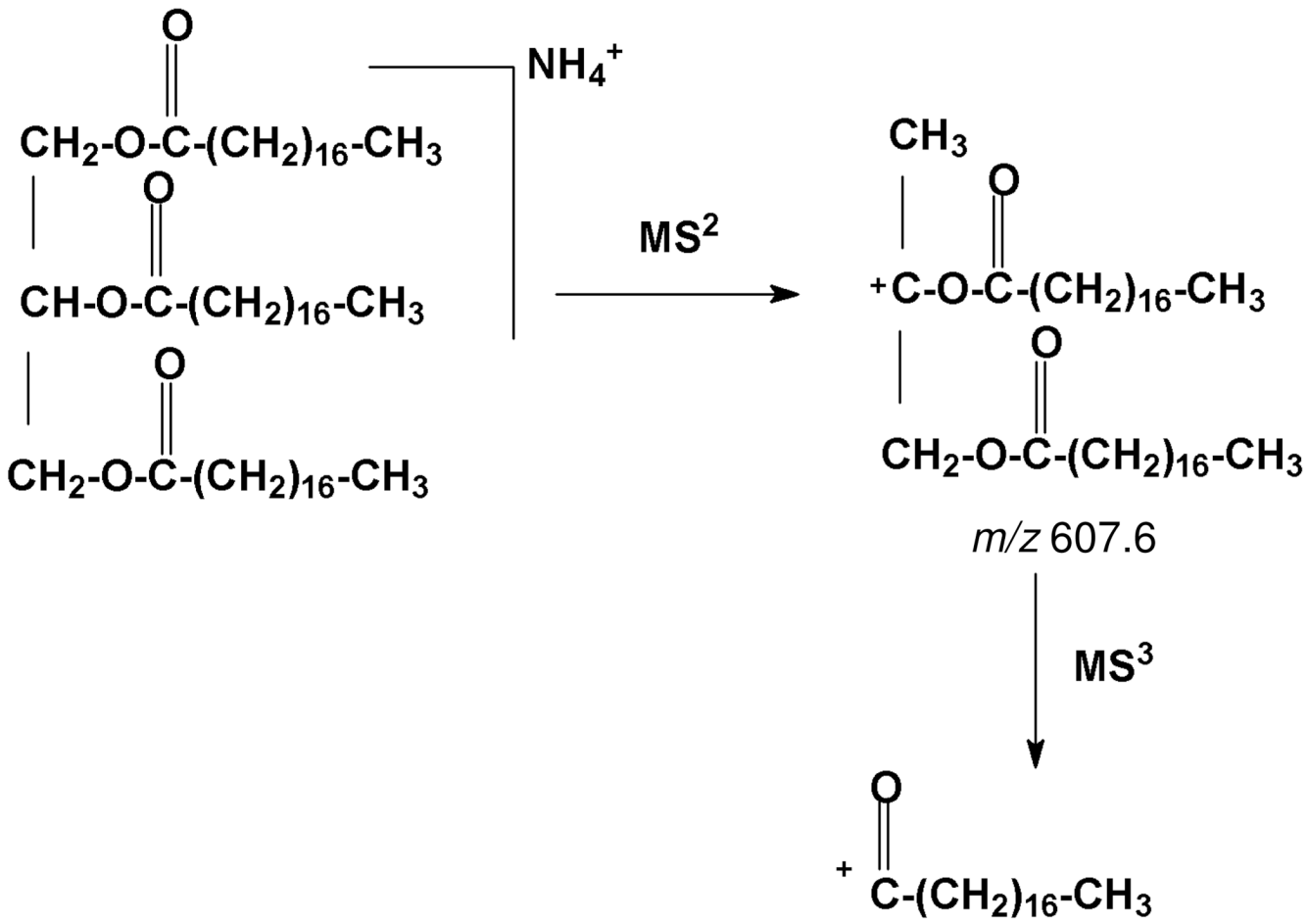

Figure 1.
MS fragmentation pathways for glycerol tristearate (tristearin).

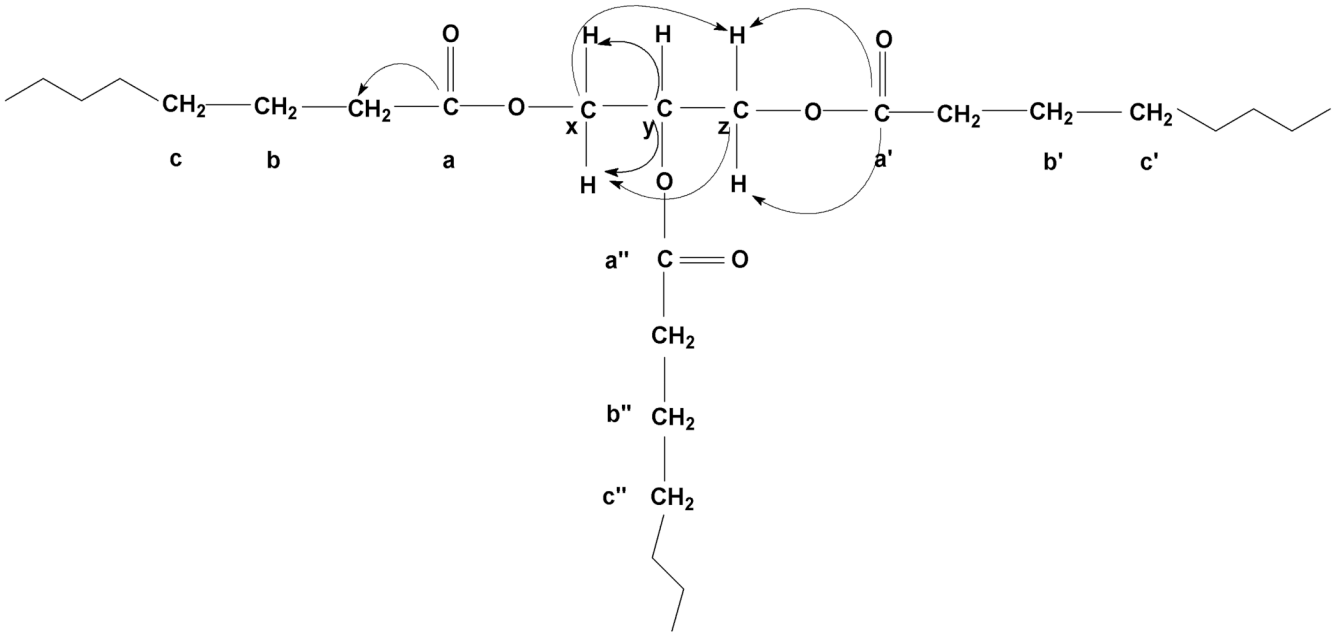

Figure 2.
Triacylglycerols identified by NMR spectroscopy. Carbons 1 and 3 are equivalent, but HMQC shows that each of them is bound to a pair of inequivalent H's. HMBC correlations used to deduce the structure are shown as C→H.

NIH-PA Author Manuscript
NIH-PA Author Manuscript
NIH-PA Author Manuscript

NIH-PA Author Manuscript

NIH-PA Author Manuscript

NIH-PA Author Manuscript

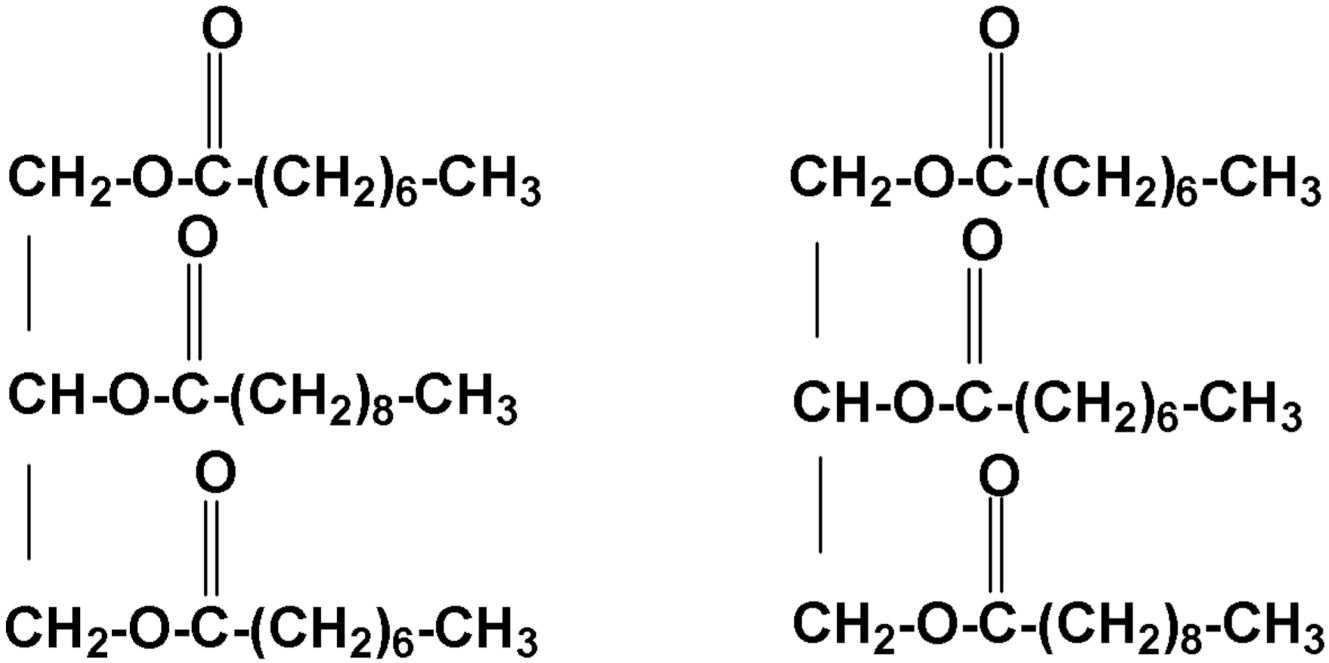

Figure 3.
Typical triglyceride structures for Compound **2** identified from 2D NMR and MS^n experiments.

NIH-PA Author Manuscript

NIH-PA Author Manuscript

NIH-PA Author Manuscript

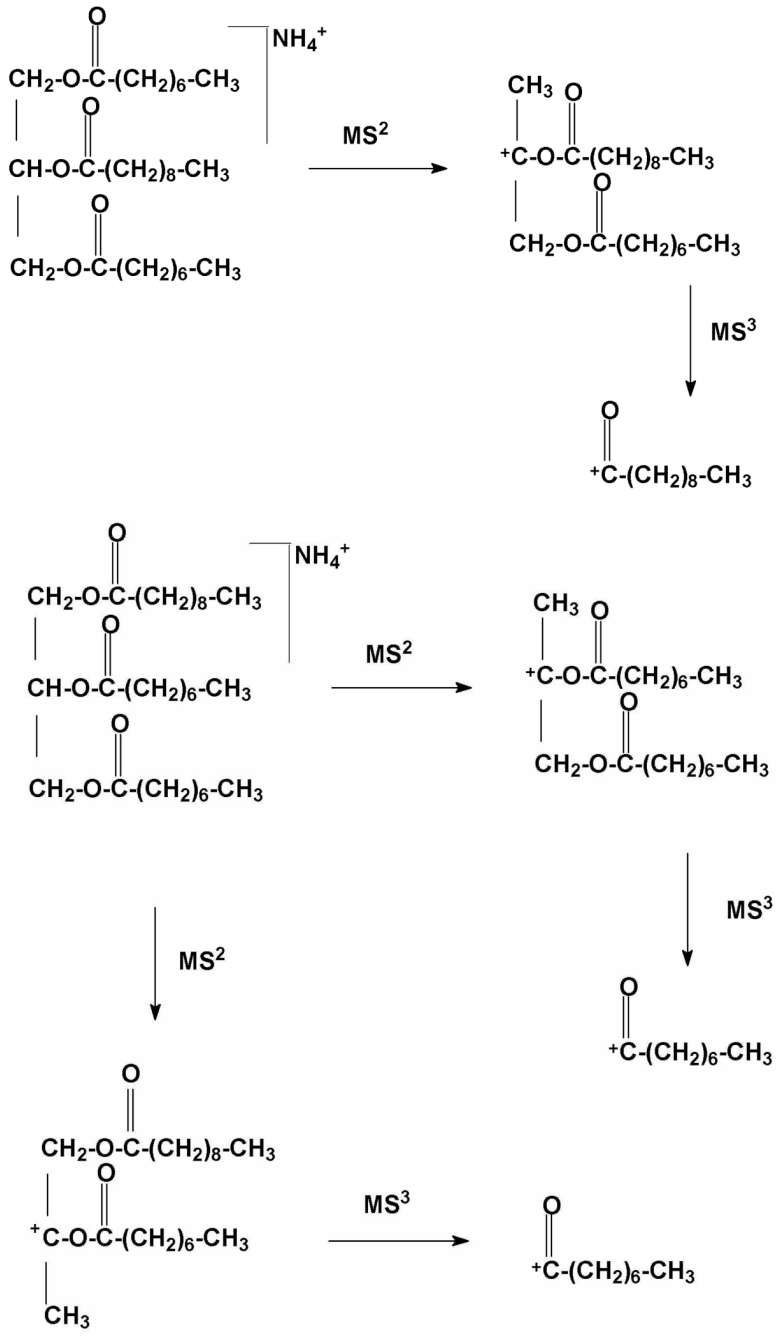

Figure 4.
MS fragmentation of successive C_8 and C_{10} acyl chains for **2**.

NIH-PA Author Manuscript

NIH-PA Author Manuscript

NIH-PA Author Manuscript

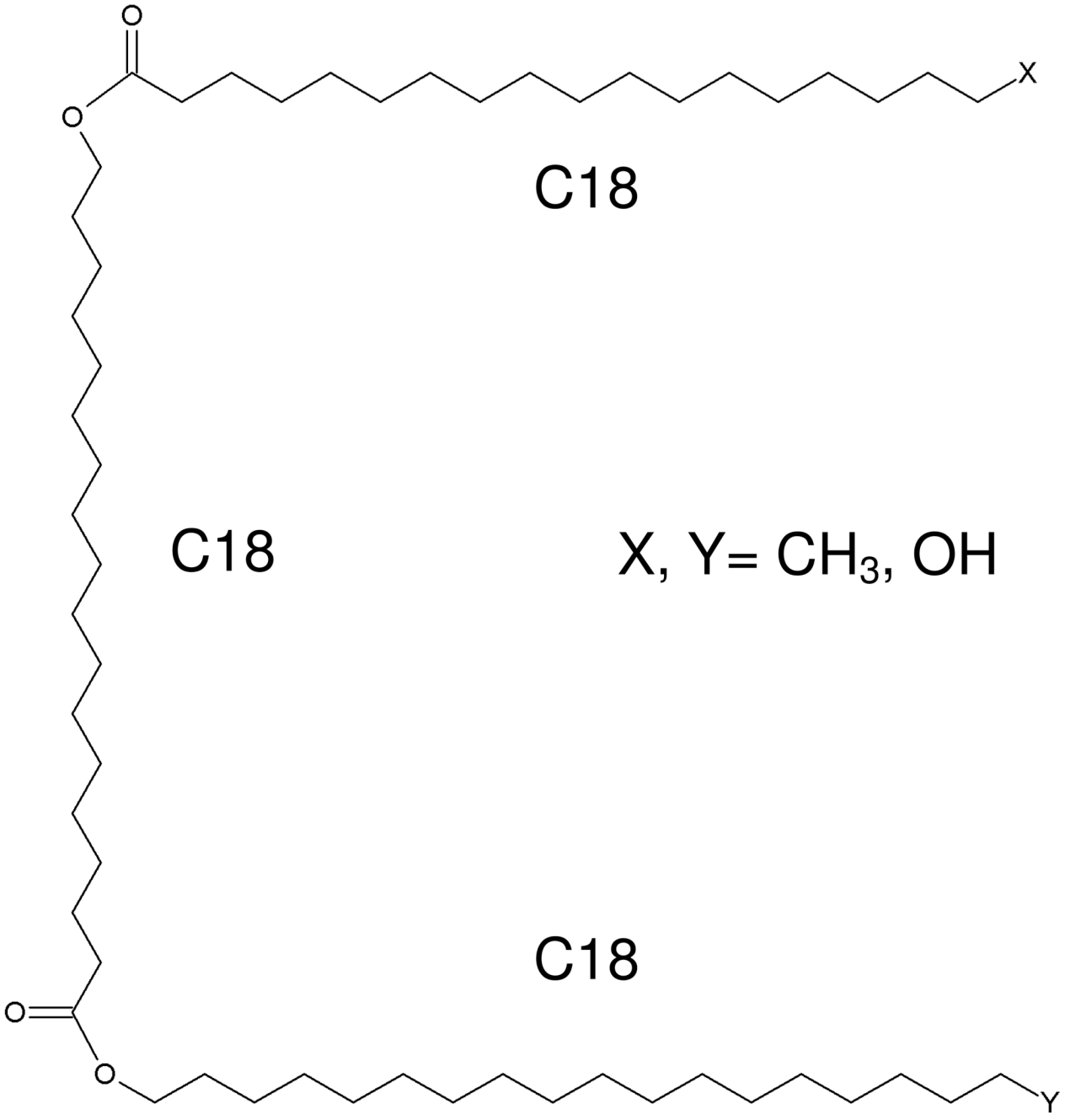

Figure 5.
Trimer esters comprising Compound **3**. (The order of the monomeric units is undetermined.)

NIH-PA Author Manuscript

NIH-PA Author Manuscript

NIH-PA Author Manuscript

Table 1

Mass spectrometric data and proposed structures for triacylglycerols (**2**)

observed ion (*m/z*), $[M+NH_4]^+$	molecular weight (M)	m[a]	probable chain-length combinations[b]	fraction number(s)
419.3	401.3	--[c]	---	**1**
488.4	470.4	9	8, 8, 8	**1, 3, 4**
516.4	498.4	10	8, 8, 10	**2**
544.4	526.4	11	8, 10, 10	**1**
600.5	582.6	13	8, 12, 12	**4**
656.5	638.7	15	12, 12, 12	**3, 4**
684.7	666.7	16	12, 12, 14	**3, 4**
740.8	722.7	18	10, 16, 16	**3, 4**
768.8	750.8	19	14, 14, 16	**3, 4**
784.8	766.8	--[c]	---	**3, 4**
796.8	778.8	20	14, 16, 16	**3, 4**
824.8	806.8	21	16, 16, 16	**4**
852.6	834.6	22	16, 16, 18	**4**
908.4	890.7	24	18, 18, 18	**4**

[a] M = A-18 = 218.03 + 28.03 m, where m is the number of chain ethylenes.

[b] Three chains with structure $C(O)O-(CH_2)_n-CH_3$. As in neutral fats, chains with even numbers of carbons and similar length were designated as most likely (23), unless demonstrated otherwise by MS^n.

[c] Ions that do not correspond to a triglyceride formula; NMR data support identification as linear aliphatic ester oligomers.

NIH-PA Author Manuscript

NIH-PA Author Manuscript

NIH-PA Author Manuscript

Table 2

NMR spectral data ($CDCl_3$) for triacylglycerols from potato wound periderm

position	functional group[a]	δ_H (ppm) [b]	δ_C (ppm) [b, c]
a, a', a''	C(O)O		173.0
y	-(C(O)O-CH_2)$_2$-**CH**-O-	5.24	68.8
x, x', z, z'	-(C(O)O-**CH_2**)$_2$-CH-O-	4.13, 4.28	61.9
b, b', b"	**CH_2**CH_2C=O	1.41	28.9
c, c', c"	**$(CH_2)_n$**	1.23	24.5
	CH_2C(O)O	2.28	34.1

[a] Nuclear spins that exhibited HMQC correlations are shown in **bold**.

[b] Referenced to internal tetramethylsilane.

[c] An ester was also present, evidenced by a **CH_2**OC(O) resonance observed in HMQC at (4.03, 64.5 ppm).

NIH-PA Author Manuscript NIH-PA Author Manuscript NIH-PA Author Manuscript

Table 3

MS spectrometric data and proposed structures for ester oligomers in compound *3*

m/z $[M+H]^+$	*m/z* $[M+NH4]^+$	*m/z* $[M-H]^-$	terminal groups	molecular weight (M)	chain-length combinations
637	654	not observed	CH_3, CH_3	636	12, 14, 14
665	682	not observed	CH_3, CH_3	664	14, 14, 14
681	--[a]	679	CH_3, OH	680	14, 14, 14
693	710	not observed	CH_3, CH_3	692	14, 14, 16
709	--	707	CH_3, OH	708	14, 14, 16
721	738	not observed	CH_3, CH_3	720	14, 16, 16
737	--	735	CH_3, OH	736	14, 16, 16
749	766	not observed	CH_3, CH_3	748	16, 16, 16
765	--	763	CH_3, OH	764	16, 16, 16
777	794	not observed	CH_3, CH_3	776	16, 16, 18 or 14, 18, 18
793	--	791	CH_3, OH	792	16, 16, 18 or 14, 18, 18
805	822.7	not observed	CH_3, CH_3	804	16, 16, 18
821	--	819	CH_3, OH	820	16, 18, 18
833	850 (weak)	not observed	CH_3, CH_3	832	18, 18, 18
849	--	847	CH_3, OH	848	18, 18, 18

[a]Not measured.

J Agric Food Chem. Author manuscript; available in PMC 2011 January 27.